Corticospinal tract location in internal capsule of human brain: diffusion tensor tractography and functional MRI study

Yun-Hee Kim[a], Dae-Shik Kim[b], Ji Heon Hong[e], Chang Hyun Park[a], Ning Hua[c], Kevin C. Bickart[d], Woo Mok Byun[f] and Sung Ho Jang[g]

[a]Department of Physical Medicine and Rehabilitation, Samsung Medical Center, Sungkyunkwan University School of Medicine, [b]Department of Anatomy and Neurobiology, [c]Biophysics, [d]Department of Anatomy for Biomedical Imaging, School of Medicine Boston University, Massachusetts, USA, [e]Department of Rehabilitation Science, Taegu University, [f]Department of Diagnostic Radiology and [g]Department of Physical Medicine and Rehabilitation, College of Medicine, Yeungnam University

Correspondence to Sung Ho Jang, MD, Associate Professor, Department of Physical Medicine and Rehabilitation, College of Medicine, Yeungnam University 317-1, Daemyungdong, Namku, Taegu 705-717, Republic of Korea
Tel: +82 053 620 3269; fax: +82 53 620 3269; e-mail: strokerehab@hanmail.net, belado@med.yu.ac.kr

Received 22 January 2008; accepted 11 March 2008

We attempted to elucidate the corticospinal tract location at the posterior limb of the internal capsule in the human brain. Ten healthy volunteers were recruited. Probabilistic mapping was performed using the functional MRI activation resulting from a hand motor task as region of interest 1 and the corticospinal tract area of the anterior pons as region of interest 2. The average location of the highest density point of the corticospinal tract was mid-posterior portion with the standard from the most medial point to the most posterior point of the lenticular nucleus. In conclusion, we demonstrated that the corticospinal tract for the hand descended through the posterior portion of the posterior limb at the mid-thalamic level. *NeuroReport* 19:817–820 © 2008 Wolters Kluwer Health | Lippincott Williams & Wilkins.

Keywords: corticospinal tract, diffusion tensor imaging, functional MRI, internal capsule

Introduction

The corticospinal tract (CST) is the most important motor pathway that functions in human motor control. The preservation or recovery of the CST is mandatory for good recovery of impaired motor function in patients with brain injury [1,2]. The accurate estimation of the CST state after brain injury would enable us to predict the sequelae of motor weakness or to set up a scientific management strategy. This information also could be useful in accurate surgical planning for patients with brain tumor or vascular anomaly. In contrast, the posterior limb of the internal capsule is an important location because this area is related to poor motor outcomes [3].

The exact location of the CST at the posterior limb of the internal capsule remains controversial, although many studies have attempted to elucidate the location of the CST at the posterior limb of the internal capsule in the human brain [4–14]. The invasive methods such as brain dissection or direct brain stimulation study have mainly been used in the past [4–9]. The development of the radiologic techniques enable us to do noninvasive research on this topic [10–14]. In particular, the diffusion tensor tractography (DTT), which is derived from diffusion tensor imaging (DTI), has the advantage of being capable of visualizing and localizing the CST at the subcortical level in three dimensions [15–19]. The validity and reliability of DTT for the CST has been demonstrated well in earlier studies [15,20,21]. In contrast, functional MRI (fMRI) is capable of precisely identifying cortical activation sites because of its excellent spatial resolution at the cortex [22]. Therefore, it seems that combined fMRI/DTT would allow more accurate localization of the CST. Few DTT studies have attempted to use fMRI results for elucidating the CST location at the posterior limb of the internal capsule [11,13].

In this study, we attempted to elucidate the CST location for the hand at the posterior limb of the internal capsule in the normal human brain, using DTT analyzed with the results of fMRI activation.

Materials and methods

Participants

Ten healthy, right-handed participants (men: 6, mean age: 28.8 years, range: 20–37 years) without an earlier history of neurological, psychiatric, or physical illness were enrolled in this study. The both hands of each participant were examined in one session using modified Edinburg Handedness Inventory for determination of handness [23]. All participants understood the purpose of this study, and provided written informed consent before participation in this experiment. This study was approved by the institutional review board of a university hospital.

Data acquisition

The blood oxygenation level-dependent (BOLD) fMRI measurement, which uses the echo planar imaging (EPI)

technique, was performed using a 1.5-T Philips Gyroscan Intera (Hoffman-LaRoche, Ltd, Best, the Netherlands) with a standard head coil. The EPI BOLD images were acquired over the same 20 axial sections, producing a total of 1200 images for each participant. Imaging parameters consisted of repetition time/echo time=2 s/60 ms, field of view=210 mm, matrix size=64 × 64, and slice thickness =5 mm. Participants were examined in a supine position with their eyes closed, and were firmly secured with the forearm pronated. For the motor task, a repetitive alternating cycle of control (rest for 21 s) and stimulation (activity for 21 s) with grasp–release hand movements at a metronome-guided frequency of 1 Hz was performed. Each of the 'control and stimulation' (42 s) tasks was repeated three times.

The DTIs were acquired using a sensitivity-encoding head coil on a 1.5-T Philips Gyroscan Intera (Hoffman-LaRoche, Ltd) with single-shot EPI with a navigator echo. Sixty contiguous slices (matrix=128 × 128, field of view=221 mm, repetition time/echo time=10726/76 ms, b=600 mm^2 s^{-1}, thickness=2.3 mm) were acquired for each of the 32 noncollinear diffusion-sensitizing gradients.

Data processing

Functional MRI data were analyzed using SPM2 software (Wellcome Department of Cognitive Neurology, London, UK) running under the MATLAB environment (The Mathworks, Natick, Massachusetts, USA). All images were preprocessed with a slice timing correction and motion realignment. These data were then coregistered and resliced using the diffusion -weighted-EPI volume with the highest signal-to-noise ratio (no diffusion weighting, b=0) as a template for each participant. The final processing was smoothed with an 8-mm isotropic Gaussian kernel. Statistical parametric maps were obtained, and voxels were considered significant at an uncorrected P less than 0.001. Activations were based on the extent of 10 voxels.

Diffusion -weighted imaging data were analyzed using BEAR [24], an in-house MATLAB-based software package (The Mathworks, Natick, Massachusetts, USA). EPI-based statistical maps were created in the SPM2 environment. The coregistration of the fMRI volumes of each participant to the diffusion dataset permitted us to directly apply the BOLD-activated maps as regions of interest (ROIs) for fiber tracking. As this study was focused on the CST, all noncortical activations were discarded. The CST related to hand motor function was determined by choosing the fibers passing through both of the ROIs (ROI 1: the activated cluster including the precentral knob, ROI 2: known anatomical CST area – blue portion of the anterior pons on the color map) (Fig. 1).

The probabilistic index of connectivity algorithm was used to track the CST [25]. This approach produces the probability density function. The probability density function was defined at each voxel within the brain to provide an estimate of confidence in the fiber tract orientation. Probabilistic fiber tracking and mapping was performed by introducing uncertainty in the local fiber orientation at all points along its propagation using the standard Monte Carlo approach. The probability value for each voxel containing axonal projections was obtained by the equation, $P=N/N$ fibers $\times 100$ (in percentage), where N is the number of fibers going through a given voxel in the fiber bundle and N fibers is the total number of fibers connecting the both ROIs. Note that many fibers that are created in the Monte Carlo tracking method and that do not reach the target ROIs are not taken into account. Probability maps are normalized to the total number of fibers, N fibers. In this study, we have an interest in the CST location at the posterior limb of the internal capsule. Therefore, the probability maps computed represent the fiber density in the bundle between the two ROIs, and provide an indication of the most likely path between the two ROIs.

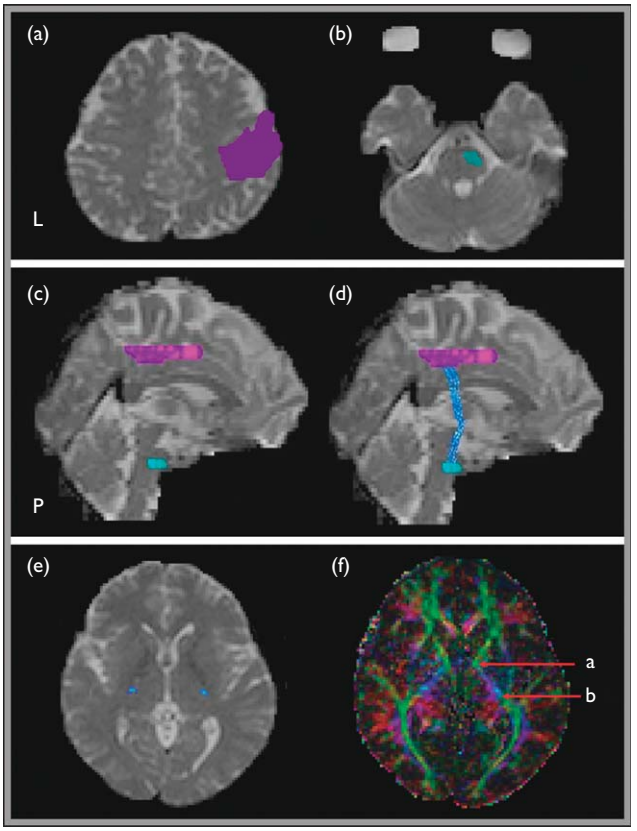

Fig. 1 The process of analysis and measurement of the corticospinal tract location. (a) Region of interest (ROI) 1: the activated area including the precentral knob, (b) ROI 2: the known corticospinal tract area of the anterior pons, (c) the sagittal view of the ROIs 1 and 2, (d) fiber tract connecting the ROIs 1 and 2, (e) probabilistic map of the corticospinal tract in the posterior limb, (f) the landmarks for measurement of the corticospinal tract location: a – the most medial point of the lenticular nucleus, b – the most posterior point of the lenticular nucleus.

Measurements of the corticospinal tract location at the posterior limb

We measured the location of the CST in the posterior limb of the internal capsule at the level of the mid-thalamus. We defined $A(x1, y1)$ as the most medial point of the lenticular nucleus, and $B(x2, y2)$ as the most posterior point of the lenticular nucleus (Fig. 1). We defined C as the CST(X, Y), and measured the anterior, posterior margin of the CST and the highest density point as the most plentiful number of fibers going through a given voxel in the CST at the posterior limb of the internal capsule. We measured the location of the CST at the posterior limb of the internal

capsule using the following equation:

$$C(\text{CST location})\% = \sqrt{\frac{(x1 - X)^2 + (y1 - Y)^2}{(x1 - x2)^2 + (y1 - y2)^2}} \times 100$$

Statistical analysis

The highest density point, the anterior margin of the CST at the posterior limb of the internal capsule, the posterior margin of the CST at the posterior limb of the internal capsule, fractional anisotropy, and the probability of tracking CST were used to perform an independent *t*-test to determine the variances between the right and left hemisphere. Results were considered significant at *P* less than 0.05.

Results

Figure 2 shows the location of the CST in the posterior limb of the internal capsule at the level of the mid-thalamus. All of the CSTs descended through the area between the most medial point of the lenticular nucleus and the most posterior point of the lenticular nucleus. The relative average location of the highest density point of the CST was 76.35% with the standard from the most medial point to the most posterior point of the lenticular nucleus (Table 1). The average anterior and posterior margins of the CST were located at 64.27 and 86.72%, respectively. The mean probability was 18.93, and the average value of fractional anisotropy was 0.61. No significant differences were observed between the hemispheres in terms of the highest density point, the anterior margin, the posterior margin, the mean probability, and the fractional anisotropy.

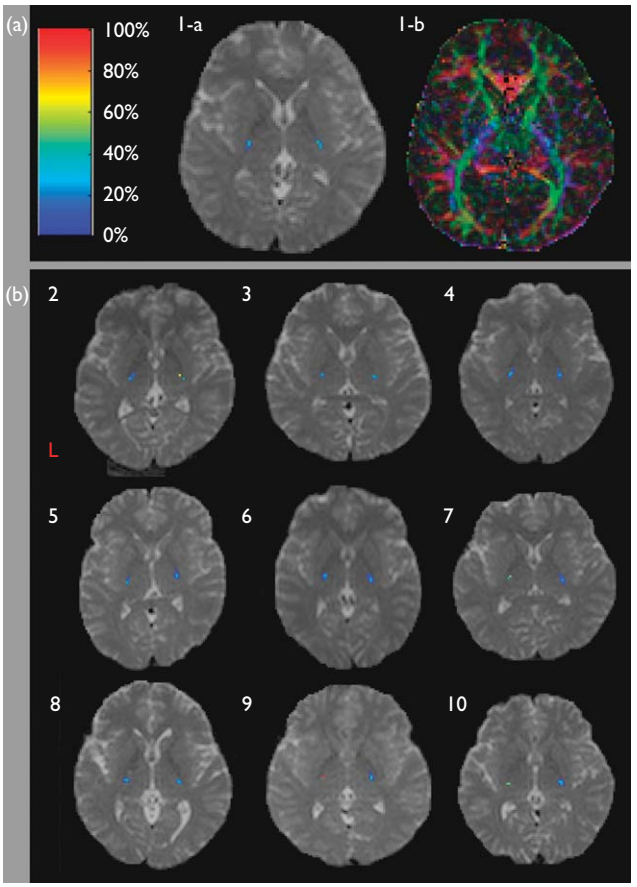

Fig. 2 The probabilistic map of the corticospinal tract in the posterior limb. Each number indicates the individual participants.

Table 1 Comparison of mean values according to the hemispheres

	Right hemisphere	Left hemisphere	Total
Highest density point (%)	76.34±5.84	76.35±6.97	76.35±6.26
Anterior margin (%)	63.78±8.23	64.76±10.23	64.27±9.05
Posterior margin (%)	88.49±5.83	84.95±8.41	86.72±7.27
Mean probability (%)	15.36±9.12	22.49±20.74	18.93±16.02
Fractional anisotropy	0.59±0.03	0.62±0.03	0.61±0.03

Values indicate mean±standard deviation.

Discussion

In this study, we attempted to investigate the location of the CST for the hand at the posterior limb of the internal capsule using the combined fMRI/DTT method. The classical concept was that the CST was located at the anterior portion of the posterior limb of the internal capsule [12]. The opinion that the CST located at the posterior portion of the posterior limb of the internal capsule, however, seems to prevail in current research studies [4]. Englander *et al.* [5] and Hanaway and Young [6] reported that the CST was located in the third quarter of the posterior limb of the internal capsule (anterior to the posterior border of the lenticular nucleus) at the mid-thalamic level and posterior half of the posterior limb of the internal capsule using an autopsy study of stroke patients. In contrast, a normal brain dissection study demonstrated that the CST entered the rostral, the posterior limb of the internal capsule at the anterior half of the posterior limb of the internal capsule in either the first or second quarter [8]. The CST progressively shifted position into the posterior half of the posterior limb of the internal capsule in the caudal portion, and passed into the third quarter. In some brains, it occupied a portion of the fourth quarter at the lower thalamic level. Another newborn brain dissection study showed that the CST was located in the middle of the posterior limb of the internal capsule, in the rostral portion at the level of the interventricular foramen, and in the posterior third of the posterior limb of the internal capsule at the level of the caudal portion at the subthalamic nucleus [9]. In 1994, a T2-weighted MRI study reported that the CST was located at the posterior portion of the posterior limb of the internal capsule [10]. After the introduction of DTT, three studies about the CST location at the posterior limb of the internal capsule were conducted [11,13,14]. Holodny *et al.* [11] demonstrated that the CST was located at the third quarter of the posterior limb of the internal capsule using DTT. The other studies were conducted to investigate the somatotopy of the hand and foot, as well as asymmetry according to handness [13,14], but not the CST location. Our results showed that the CST was located at an average of 76.35% in terms of the highest density point and 64.27–86.72% in terms of the CST location range at the posterior limb of the internal capsule. On the whole, the results of this study seem to coincide with those of previous studies. Direct comparison, however, would be impossible because the earlier studies did not define the exact boundary of the posterior limb of the internal capsule and their analyzed area, or did not declare the axial cutting level [4–11,13,14]. We measured the relative distance from the most medial point to the most

posterior point of the lenticular nucleus at the mid-thalamic level for easy clinical application. The other reason we compare our results with those of earlier studies is that our study was designed only for the CST of hand motor function, but most of the earlier studies were designed for the whole CST.

DTT seems to be a revolutionary tool for the investigation of the neural pathways at the subcortical level. DTT can, however, lead to erroneous results because this technique can be operator-dependent, or can show mathematical results irrespective of real anatomy [11,12,19]. In contrast, the combined method with fMRI has an advantage in that it allows us to obtain anatomical data derived from functional data. In this study, we transferred the fMRI activation resulting from a hand motor task to the DTI analysis program [24]. We used the cortical activation as an ROI and the CST area of the pons as the anatomic location of the CST, which is not in dispute as another ROI. There have been two DTT studies conducted to determine the location of the CST to try to combine with fMRI, as in this study [11,13]. These studies, however, have a limitation in that fMRI was performed only for some of the participants [11], or drew the fMRI activation area by hand [11,13]. Therefore, as far as we know, this is the first study to demonstrate the CST location in the human brain using DTT analyzed by the fMRI activation results.

Conclusion

In conclusion, we demonstrated that the CST for the hand descended through the posterior portion of the posterior limb of the internal capsule at the mid-thalamic level. Therefore, we think that this combined method of fMRI/DTT could be useful for investigating the anatomy of the human brain.

Acknowledgements

This research was supported by the Samsung Medical Center Clinical Research Development Program (CRDP) (CRS105-04-1) and a grant from a KOSEF grant funded by the Korean government (MOST) (No. M10644000022-06N4400-02210).

References

1. Hallett M, Wassermann EM, Cohen LG, Chmielowska J, Gerloff C. Cortical mechanisms of recovery of function after stroke. *Neurorehabilitation* 1998; **10**:131–142.
2. Ahn YH, Ahn SH, Kim H, Hong JH, Jang SH. Can stroke patients walk after complete lateral corticospinal tract injury of affected hemisphere? *Neuroreport* 2006; **17**:987–990.
3. Shelton FN, Reding MJ. Effect of lesion location on upper limb motor recovery after stroke. *Stroke* 2001; **32**:107–112.
4. Bertrand G, Blundell J, Musella R. Electrical exploration of the internal capsule and neighbouring structures during stereotaxic procedures. *J Neurosurg* 1965; **22**:333–343.
5. Englander RN, Netsky MG, Adelman LS. Location of human pyramidal tract in the internal capsule: anatomic evidence. *Neurology* 1975; **25**:823–826.
6. Hanaway J, Young RR. Localization of the pyramidal tract in the internal capsule of man. *J Neurol Sci* 1977; **34**:63–70.
7. Hardy TL, Bertrand G, Thompson CJ. The position and organization of motor fibers in the internal capsule found during stereotactic surgery. *Appl Neurophysiol* 1979; **42**:160–170.
8. Ross ED. Localization of the pyramidal tract in the internal capsule by whole brain dissection. *Neurology* 1980; **30**:59–64.
9. Kretschmann HJ. Localisation of the corticospinal fibres in the internal capsule in man. *J Anat* 1988; **160**:219–225.
10. Yagishita A, Nakano I, Oda M, Hirano A. Location of the corticospinal tract in the internal capsule at MR imaging. *Radiology* 1994; **191**:455–460.
11. Holodny AI, Gor DM, Watts R, Gutin PH, Ulug AM. Diffusion-tensor MR tractography of somatotopic organization of corticospinal tracts in the internal capsule: initial anatomic results in contradistinction to prior reports. *Radiology* 2005; **234**:649–653.
12. Holodny AI, Watts R, Korneinko VN, Pronin IN, Zhukovskiy ME, Gor DM, *et al*. Diffusion tensor tractography of the motor white matter tracts in man: current controversies and future directions. *Ann N Y Acad Sci* 2005; **1064**:88–97.
13. Ino T, Nakai R, Azuma T, Yamamoto T, Tsutsumi S, Fukuyama H. Somatotopy of corticospinal tract in the internal capsule shown by functional MRI and diffusion tensor images. *Neuroreport* 2007; **18**:665–668.
14. Westerhausen R, Huster RJ, Kreuder F, Wittling W, Schweiger E. Corticospinal tract asymmetries at the level of the internal capsule: is there an association with handedness? *Neuroimage* 2007; **37**:379–386.
15. Mori S, Crain BJ, Chaco VP, van Zijl PC. Three-dimensional tracking of axonal projections in the brain by magnetic resonance imaging. *Ann Neurol* 1999; **45**:265–269.
16. Ronen I, Ugurbil K, Kim DS. How does DWI correlate with white matter structures. *Magn Reson Med* 2005; **54**:317–323.
17. Ahn YH, You SH, Randolph M, Kim SH, Ahn SH, Byun WM, *et al*. Peri-infarct reorganization of motor function in patients with pontine infarct. *Neurorehabilitation* 2006; **21**:233–237.
18. Jang SH, Kim YH, Kwon YH, You S, Han BS, Byun WM. Restoration of corticospinal tract compressed by hematoma: a diffusion tensor tractography study. *Arch Neurol* 2006; **63**:140–141.
19. Lee SK, Kim DI, Kim J, Kim DJ, Kim HD, Kim DS, *et al*. Diffusion-tensor MR imaging and fiber tractography: a new method of describing aberrant fiber connections in developmental CNS anomalies. *Radiographics* 2005; **25**:53–65.
20. Ciccarellia O, Parkerb GJM, Toosya AT, Wheeler-Kingshott CA, Barker GJ, Boulby PA, *et al*. Thompson from diffusion tractography to quantitative white matter tract measures: a reproducibility study. *Neuroimage* 2003; **18**:348–359.
21. Burgel U, Amunts K, Hoemke L, Mohlberg H, Gilsbach JM, Zilles K. White matter fiber tracts of the human brain: three-dimensional mapping at microscopic resolution, topography and intersubject variability. *Neuroimage* 2006; **29**:1092–1105.
22. Guye M, Parker GJ, Symms M, Boulby P, Wheeler-Kingshott CA, Salek-Haddadi A, *et al*. Combined functional MRI and tractography to demonstrate the connectivity of the human primary motor cortex in vivo. *Neuroimage* 2003; **19**:1349–1360.
23. Oldfield RC. The assessment and analysis of handedness: the Edinburgh inventory. *Neuropsychologia* 1971; **9**:97–113.
24. Upadhyay J, Ducros M, Knaus TA, Lindgren KA, Silver A, Tager-Flusberg H, *et al*. Function and connectivity in human primary auditory cortex: a combined fMRI and DTI study at 3 Tesla. *Cereb Cortex* 2007; **17**:2420–2432.
25. Parker GJ, Haroon HA, Wheeler-Kingshott CA. A framework for a streamline-based probabilistic index of connectivity (PICo) using a structural interpretation of MRI diffusion measurements. *J Magn Reson Imaging* 2003; **18**:242–254.